

# Paramagnetic Rim Lesions in Pediatric Multiple Sclerosis and Their Association With Brain Tissue Atrophy

Riccardo Nistri,<sup>1,2,\*</sup> Ermelinda De Meo,<sup>1,\*†</sup> Nee Na Kim,<sup>1,2</sup> Valeria Pozzilli,<sup>1,3</sup> Philip Goebel,<sup>1,4</sup> Mario Sa,<sup>5</sup> Sithara Ramdas,<sup>5</sup> Amitav Parida,<sup>6</sup> Sukhvir Wright,<sup>6,7</sup> Evangeline Wassmer,<sup>6,7</sup> Michael Eyre,<sup>8,9</sup> Ming Lim,<sup>10,8</sup> Thomas Rossor,<sup>10,8</sup> Cheryl Hemingway,<sup>2</sup> Asthik Biswas,<sup>11</sup> Sniya Sudhakar,<sup>11</sup> Kshitij Mankad,<sup>11</sup> Arman Eshaghi,<sup>1,4</sup> Frederik Barkhof,<sup>12,13</sup> Olga Ciccarelli,<sup>1,14</sup> and Yael Hacohen<sup>1,2,†</sup>

## Correspondence

Dr. De Meo  
ermelinda.demeo@unifi.it  
or Dr. Hacohen  
y.hacohen@ucl.ac.uk

*Neurol Neuroimmunol Neuroinflamm* 2026;13:e200506. doi:10.1212/NXI.000000000200506

## Abstract

### Background and Objectives

Paramagnetic rim lesions (PRLs), visible on susceptibility-based imaging (SbI), reflect chronic active inflammation in multiple sclerosis (MS). In adult-onset MS, PRLs are associated with a more aggressive disease course. The objectives of this study were to assess the prevalence of PRLs in children with MS and to examine how baseline PRL count relates to clinical disability and brain tissue volume loss, both cross-sectionally and over short-term follow-up.

### Methods

We retrospectively analyzed pediatric patients from 4 UK tertiary neuroimmunology centers who met the 2017 McDonald diagnostic criteria and had 3D T1-weighted, T2-weighted, fluid-attenuated inversion recovery, and SbI MRI available. PRLs were identified per North American Imaging in MS criteria and anatomically classified. Brain volumes were segmented using Mindglide, with z-scores derived from NIH normative data. Associations between baseline PRL burden, clinical variables, and brain volumes were assessed using univariable and multivariable stepwise regression. Linear mixed-effects models evaluated the predictive value of baseline PRL burden on longitudinal brain volume changes.

### Results

Fifty-four patients (mean age  $14.0 \pm 2.2$  years; 75.9% female) were included. At least 1 PRL was seen in 74.1% of patients, with a median number of 2 PRLs (interquartile range [IQR] = 0–6), predominantly in periventricular regions, and accounting for 25% of total T2-weighted hyperintense lesions. In multivariable Poisson regression, at baseline, shorter disease duration (incidence rate ratio [IRR] = 0.987, 95% CI 0.975–0.999,  $p = 0.035$ ), and greater number (IRR 1.045, 95% CI 1.035–1.054,  $p < 0.001$ ) and volume (IRR 1.018, 95% CI 1.004–1.032,  $p = 0.012$ ) of T2-hyperintense lesions were associated with higher PRL count. Cross-sectionally, a higher PRL count was associated with lower cortical ( $\beta = -0.139$ , 95% CI  $-0.231$  to  $-0.047$ ,  $p = 0.016$ ) and deep ( $\beta = -0.096$ , 95% CI  $-0.166$  to  $-0.026$ ,  $p = 0.032$ ) gray matter volume z-scores. No significant association was observed between clinical disability and PRL count. In 45 patients followed up for a median 17 months (IQR 12–24), a higher baseline PRL count predicted greater deep gray matter volume loss over time ( $\beta = -0.020$ , 95% CI  $-0.034$  to  $-0.006$ ,  $p = 0.036$ ).

\*These authors contributed equally to this work as co-first authors.

†These authors contributed equally to this work as co-corresponding authors.

<sup>1</sup>Queen Square MS Center, Department of Neuroinflammation, UCL Queen Square Institute of Neurology, Faculty of Brain Sciences, University College London, United Kingdom; <sup>2</sup>Department of Neurology, Great Ormond Street Hospital for Children, University College London, United Kingdom; <sup>3</sup>Unit of Neurology, Neurophysiology and Neurobiology, Department of Medicine and Surgery, Campus Bio-Medico University, Rome, Italy; <sup>4</sup>UCL Hawkes Institute, Department of Medical Physics and Bioengineering, University College London, United Kingdom; <sup>5</sup>Department of Paediatrics, Department of Paediatric Neurology, John Radcliffe Hospital, University of Oxford, United Kingdom; <sup>6</sup>Department of Pediatric Neurology, Birmingham Children's Hospital, Birmingham, United Kingdom; <sup>7</sup>Institute of Health and Neurodevelopment, College of Health and Life Sciences, Aston University, Birmingham, United Kingdom; <sup>8</sup>Children's Neurosciences, Evelina London Children's Hospital at Guy's and St Thomas' National Health Service Foundation Trust, London; United Kingdom; <sup>9</sup>Departments of Imaging Physics and Engineering and Early Life Imaging, School of Biomedical Engineering and Imaging Sciences, King's College London, United Kingdom; <sup>10</sup>Women and Children's Department, Faculty of Life Sciences and Medicine, Kings College Hospital, London, United Kingdom; <sup>11</sup>Department of Radiology, Great Ormond Street Hospital for Children, London, United Kingdom; <sup>12</sup>Department of Radiology and Nuclear Medicine, Amsterdam UMC, Vrije Universiteit, the Netherlands; <sup>13</sup>Queen Square Institute of Neurology and Centre for Medical Image Computing, University College London, United Kingdom; and <sup>14</sup>NIHR (National Institute for Health and Care Research) UCLH BRC (Biomedical Research Centre), London, United Kingdom.

The Article Processing Charge was funded by University College of London.

This is an open access article distributed under the terms of the Creative Commons Attribution-Non Commercial-No Derivatives License 4.0 (CCBY-NC-ND), where it is permissible to download and share the work provided it is properly cited. The work cannot be changed in any way or used commercially without permission from the journal.

Copyright © 2025 The Author(s). Published by Wolters Kluwer Health, Inc. on behalf of the American Academy of Neurology.

e200506(1)

MORE ONLINE

Supplementary Material

## Glossary

**DMT** = disease-modifying treatment; **EDSS** = Expanded Disability Status Scale; **FLAIR** = fluid-attenuated inversion recovery; **IQR** = interquartile range; **IRR** = incidence rate ratio; **MS** = multiple sclerosis; **POMS** = pediatric-onset MS; **PRL** = paramagnetic rim lesion; **SbI** = susceptibility-based imaging; **SWI** = susceptibility-weighted imaging.

---

## Discussion

PRLs are common in pediatric MS and are linked to greater lesion burden and gray matter atrophy. These findings suggest that PRLs are promising imaging biomarkers of more severe brain tissue damage although their ability to predict future disability requires confirmation in longer term studies.

---

## Introduction

Pediatric-onset MS (POMS) is associated with a higher relapse rate and rapid MRI lesion accrual early in the disease course.<sup>1</sup> Despite the better recovery from relapses<sup>2</sup> and lower short-term disability, POMS is associated with worse long-term cognitive and physical disability compared with adult-onset disease.<sup>3</sup> It is also linked to reduced brain growth, followed by atrophy,<sup>4</sup> although MRI-based brain volume measures remain limited to research settings.

In recent years, chronic active lesions have been recognized as *in vivo* biomarkers of smouldering inflammatory activity,<sup>5</sup> one of the main contributors to disability progression in MS.<sup>6,7</sup> The umbrella term “chronic active lesions” includes both slowly evolving lesions and paramagnetic rim lesions (PRLs).<sup>8</sup> While the identification of slowly evolving lesions requires at least 3 MRI time points and advanced image processing techniques,<sup>9</sup> PRLs can be detected from a single MRI acquisition, making them a more accessible and clinically feasible biomarker for routine use, although the use of specific iron-sensitive sequences may require longer acquisition time.

PRLs are characterized by a rim of activated microglia or macrophages at the lesion edge,<sup>10</sup> identified using susceptibility-based imaging (SbI).<sup>11</sup> PRLs can be detected in around 60% of patients with MS, with a lower prevalence in patients with relapsing-remitting MS (RRMS) compared with progressive MS.<sup>7,12</sup> In adult MS, the presence of PRLs has been associated with disability progression, particularly when 4 or more PRLs are identified.<sup>13</sup> Furthermore, emerging evidence suggested that PRLs may serve not only as prognostic indicators but also as potential diagnostic biomarkers.<sup>14</sup> Only few studies have been conducted in pediatric patients, showing the presence of at least 1 PRL in the 69%–92% of pediatric patients with MS, with a specificity for MS compared with myelin oligodendrocyte glycoprotein-associated diseases and other acquired demyelinating syndromes.<sup>15–17</sup>

The aim of this study was to evaluate whether PRL count in POMS (1) correlates with clinical disability and brain tissue volume measures and (2) predicts longitudinal outcomes, as

reflected by changes in Expanded Disability Status Scale (EDSS) scores and brain tissue volume loss over follow-up time.

## Methods

### Standard Protocol Approvals, Registrations, and Patient Consents

This study was approved by the Great Ormond Street Hospital Research and Development Department (reference: 16NC10). Because the data analysis was retrospective and no additional information was gathered beyond what was necessary for the standard medical care of the patients, informed written consent from participants was not required prior to their inclusion in the study.

### Participants and Inclusion Criteria

This retrospective analysis included pediatric patients with MS from 4 tertiary pediatric neuroimmunology centers in the United Kingdom: Great Ormond Street Hospital for Children, Evelina London Children’s Hospital, Birmingham Children Hospital, and Oxford University Trust. Inclusion criteria were as follows: (1) MS onset before age 18 years, (2) diagnosis of MS according to the 2017 diagnostic criteria<sup>18</sup>; (3) brain MRI including 3D T1-weighted, T2-weighted, fluid-attenuated inversion recovery (FLAIR), and susceptibility-weighted imaging (SWI) or other SbI sequences.

Because imaging was performed in routine clinical practice, baseline was defined as each patient’s earliest scan meeting our inclusion criteria. To ensure that PRLs reflected chronic pathology rather than transient inflammation and to minimize the impact of acute phenomena (such as vasogenic edema) on brain volume measurements, we included only MRI scans performed at least 4 weeks after a clinical attack.

For longitudinal analyses, patients were required to have a follow-up MRI performed at least 6 months after their baseline scan, with no intervening relapses. While baseline SWI/SbI was mandatory for PRL detection, equivalent susceptibility-based sequences were not required on follow-up; follow-up scans needed only the standard structural

sequences (3D T1-weighted, T2-weighted, and FLAIR) to assess volumetric change.

## Data Collection

Clinical data, including demographics and disease characteristics (i.e., age at onset, sex, treatment history, and EDSS score at the time of MRI), were retrospectively reviewed from patients' electronic medical records. EDSS assessments included in this study were conducted within 3 months of MRI acquisition, in the absence of an acute clinical relapse, and at least 4 weeks after any prior relapse.

## MRI Acquisition

MRI scans were acquired as part of the routine clinical care in the National Health Service (NHS), using either 3T or 1.5T scanners, and included the following sequences: (1) 2D or 3D FLAIR and T2-weighted images for lesion detection and segmentation; (2) SWI—a high-resolution 3D gradient-echo sequence that combines magnitude images with high-pass-filtered phase data—as well as other SBI techniques (e.g., T2\*-weighted gradient-echo (GRE) magnitude, multiecho 3D GRE for R2\* mapping, and unfiltered phase images); (3) 3D T1-weighted images for brain volume quantification; (4) postcontrast T1-weighted images to detect contrast-enhancing lesions (whenever available). The MRI acquisition protocol is presented in eTable 1.

## MRI Analysis

T2-hyperintense lesions were identified on T2-FLAIR images, and the presence of PRLs was assessed on coregistered SBI and related phase maps. The evaluation of PRLs was performed by consensus of 2 raters blinded to the participant's clinical data, following the North American Imaging in MS Cooperative guidelines.<sup>19</sup> PRLs were classified according to location as follows: periventricular (with 1 edge in contact with a ventricle), deep white matter, juxtacortical (with 1 edge in contact with the cortex), or other.

The 3D T1-weighted and FLAIR images were segmented using Mindglide,<sup>20</sup> to, respectively, obtain total intracranial volume, brain tissue -whole brain, white matter (WM), cortical gray matter (GM), and deep GM- volumes, and T2 lesion volumes. Brain volumetric measures were normalized by dividing them by the total intracranial volume.

## z-Score Computation

To overcome the difficulty of obtaining longitudinal MRI scans for normative brain volume modeling from pediatric healthy controls, we selected a group of 317 pediatric healthy children (HC) from an National Institute of Health (NIH)-funded MRI Study of Normal Brain Development (NIH HC) with longitudinal MRI assessments for brain volume quantification (median follow-up: 3.6, range = 0.9, 5.4 years).<sup>21</sup> The data from the NIH-funded MRI Study of Normal Brain Development were downloaded in August 2023. MRI data from all available healthy participants were initially retrieved, followed by a quality check to assess motion and other artifacts.

Among the 317 NIH HC participants deemed suitable for analysis, 163 had 2 scans (with a median interval of 2 years between the first and second scan, ranging from 0.9 to 4.3 years) while 154 had 3 scans (with a median interval of 3.9 years between the first and third scan, ranging from 2.0 to 5.4 years).

To estimate age-specific and sex-specific brain and gray matter developmental trajectories, the following linear mixed-effects model was applied to the normalized whole brain and regional gray matter volumes of the healthy participants:<sup>22</sup>

$$V_{ij} = \beta_0 + b_{i0} + (\beta_1 + b_{i1})\text{Age}_{ij} + \beta_2\text{Sex}_i + \beta_3\text{Age}_{ij} * \text{Sex}_i + \beta_4\text{Age}_{ij}^2 + \varepsilon_{ij}$$

Here,  $V_{ij}$  represents the volume of the whole brain or of a specific GM region for the participant  $i$  at the age  $j$ .

To estimate deviations from the expected maturation trajectories of the different brain regions, we calculated z-scores for the whole brain and each brain tissue at every time point. As detailed in previous studies,<sup>22,23</sup> z-scores were computed by subtracting the mean and dividing by the SD, which was estimated from the variance-covariance matrix of the fixed effects and the residual variance of the random effects, using the age and sex of each participant.

## Statistical Analysis

Pediatric patients with MS were grouped according to the presence of PRLs (PRLs + or PRLs-). Between-group comparisons of demographic, clinical, and MRI parameters were conducted using the Pearson  $\chi^2$  test, Mann-Whitney  $U$  test, 2-sample  $t$  test, and linear models, as appropriate. Associations between PRL count and demographic, clinical, and MRI variables were examined using generalized linear models with a Poisson distribution and a log link function. To identify independent predictors of PRL count, a stepwise multivariable Poisson regression approach was applied, combining forward selection and backward elimination. At each step, variables were considered for inclusion or removal based on likelihood ratio tests, using a  $p$  value threshold of 0.15.<sup>1</sup> Multicollinearity was assessed using variance inflation factors. Model assumptions—such as the linearity of the log-transformed outcome with respect to predictors, the absence of overdispersion, and the appropriateness of the specified link function—were evaluated using diagnostic plots and goodness-of-fit tests.

Linear regression models were used to examine the association between PRL count and both clinical disability and brain volume z-scores. To assess changes in clinical disability and brain tissue volumes over the follow-up period and their association with PRLs as a continuous variable, linear mixed-effects models were used including a random intercept for each patient. In both sets of models, age, sex, disease duration, disease-modifying treatment (DMT) (anti-CD20; other DMTs, namely interferon- $\beta$  preparations and fingolimod; or no DMTs), and T2-hyperintense lesion volume were included as covariates.

All statistical analyses were conducted using R version 4.4.1. Where appropriate, false discovery rate correction was applied to account for multiple comparisons. Statistical significance was defined as  $p < 0.05$ .

## Data Availability

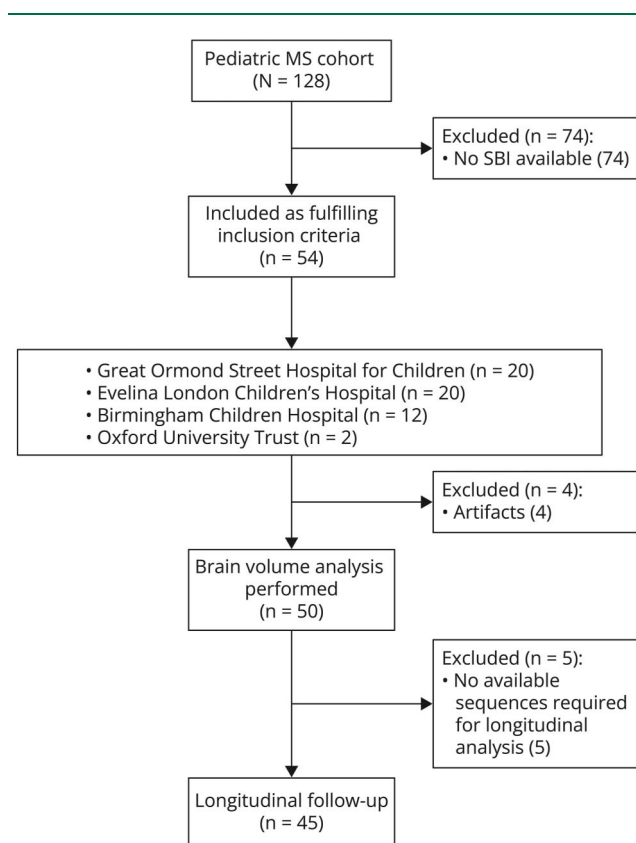
Any data not presented in the article will be made available on request to any senior (tenured) investigator.

## Results

### Cohort Demographics and Clinical and MRI Features at Baseline

A total of 54 patients fulfilled the inclusion criteria. The study flowchart summarizes cohort selection (Figure 1). Patients' demographics are summarized in Table 1. Forty-one patients were female (75.9%), and the mean age at the time of first SBI phase scan was  $14.0 \pm 2.2$  years. The median disease duration was 7 months (Interquartile range [IQR] 2–22).

**Figure 1** Flowchart of Pediatric Multiple Sclerosis Cohort Selection



This flowchart illustrates the stepwise inclusion and exclusion of pediatric patients with multiple sclerosis (MS) in our study. Beginning with the initial pool of 128 screened patients (oval), those meeting our predefined inclusion criteria ( $n = 54$ ) were retained while 74 were excluded for lack of suitable baseline imaging. After quality assurance of MRI scans, 50 patients remained for brain volume analysis and of these, 45 completed the required longitudinal follow-up interval.

### Frequency and Localization of PRLs

Forty patients (74.1%) had at least 1 PRL. An example of PRL is shown in Figure 2. The median of PRLs per patient was 2 [IQR = 0–6], and the median T2 lesions per patient was 11 (IQR = 5.25–24.25); PRLs represented 24.1% of the total number of T2 lesions per patient. In addition, PRLs represented 25% (217/865) of the total number of T2 lesions in all participants. PRLs were predominantly located in the periventricular area ( $n = 119$ ), followed by the subcortical area ( $n = 47$ ), deep white matter ( $n = 41$ ), and juxtacortical region ( $n = 8$ ).

### Association of Clinical and MRI Variables With PRL Count at Baseline

In univariable Poisson regression models, a higher number of PRLs was associated with greater T2-FLAIR lesion count [incidence rate ratio (IRR) = 1.041, 95% CI 1.034–1.049,  $p < 0.001$ ], total T2-FLAIR lesion volume (IRR 1.029, 95% CI 1.018–1.040,  $p < 0.001$ ), and lower brain volume z-scores (IRR 0.909, 95% CI 0.850–0.973,  $p = 0.006$ ). A lower number of PRLs was associated with treatment with anti-CD20 (IRR = 0.640, 95% CI 0.447–0.917,  $p = 0.015$ ). Age and disease duration were not associated with PRL count.

Multivariable stepwise Poisson regression analysis showed that higher T2-FLAIR lesion count (IRR 1.045, 95% CI 1.035–1.054,  $p < 0.001$ ) and volume (IRR 1.018, 95% CI 1.004–1.032,  $p = 0.012$ ) were both independently associated with an increased number of PRLs. Shorter disease duration was associated with greater PRL count (IRR 0.987, 95% CI 0.975–0.999,  $p = 0.035$ ). Table 2 summarizes results from both univariate and multivariable analyses.

### Association of PRLs With Clinical Disability and Brain Tissue Volumes

No association was found between PRL count and EDSS scores. Among the 50 patients whose scans fulfilled the inclusion criteria for the brain volume analysis (4 patients were excluded because of artifacts), a higher PRL count was associated with lower deep gray matter ( $\beta = -0.079$ , 95% CI  $-0.151$  to  $-0.008$ ,  $p = 0.029$ ) and cortical gray matter ( $\beta = -0.128$ , 95% CI  $-0.216$  to  $-0.040$ ,  $p = 0.007$ ) volume z-scores in linear regression models (eTable 2).

### Changes Over Time in Clinical Disability and Brain Tissue Volumes

Forty-five patients had longitudinal clinical evaluation and MRI scans, with a median of 3 scans (IQR = 3–4) and a median interval of 17 months (IQR 12–24) between the first and last scan. No new T2-hyperintense lesions were detected on any follow-up scan. We did not observe any change in the EDSS score over follow-up time while we observed reductions in brain ( $\beta = -0.342$ , 95% CI  $-0.496$  to  $-0.187$ ,  $p < 0.001$ ), deep gray matter ( $\beta = -0.127$ , 95% CI  $-0.219$  to  $-0.035$ ,  $p = 0.007$ ), and cortical gray matter ( $\beta = -0.266$ , 95% CI  $-0.386$  to  $-0.145$ ,  $p < 0.001$ ) volume z-scores (Table 3).

**Table 1** Demographic, Clinical, and MRI Characteristics of PRL-Positive vs PRL-Negative Pediatric Patients With MS at Time of MRI

	PRLs +	PRLs-	p Value
Number of patients	40	14	
Mean age (SD) (y)	14 (13.75–16)	14 (12.25–15)	0.560
Sex (F:M)	30:10	11:3	0.999
Median disease duration (IQR) (mo)	7 (1–23.5)	8 (3.25–20.25)	0.823
Number of previous relapses (median, IQR)	1(1–2)	1 (1–2)	0.31
Number of patients on DMT (%)	16 (40)	6 (43)	0.998
Number of patients on anti-CD20 (%)	13 (81.3)	3 (50)	0.350
Median EDSS score (IQR)	1 (1–2)	1 (0–1.5)	0.787
Total number of WM lesions (median, IQR)	18 (7–27)	5.5 (2–7)	<0.001
Mean T2-hyperintense lesion volume (SD) (mL)	6.4 (5.3)	9.4 (9.0)	0.094
Median number of PRLs (median, IQR)	4 (2–7.5)	0 (0)	
Mean normalized brain volume z-score (SD)	-2.74 (1.71)	-2.21 (2.21)	0.284
Mean cortical gray matter volume z-score (SD)	-2.68 (1.09)	-2.27 (1.85)	0.170
Mean deep gray matter volume z-score (SD)	-1.25 (1.20)	-2.14 (1.97)	0.061
Mean white matter volume z-score (SD)	-0.79 (1.93)	-0.01 (2.85)	0.754
Longitudinal evaluation (n = 45)	PRLs+ (n = 31)	PRLs- (n = 14)	
Delta EDSS score	0.00 ± 0.00	0.00 ± 0.00	NA
Delta lesion volume (SD) [ml]	0.21 ± 2.29	0.81 ± 3.62	0.951
Delta brain volume z-scores	0.04 ± 1.47	-0.30 ± 2.17	0.470
Delta cortical gray matter volume z-scores	0.14 ± 1.38	0.44 ± 0.97	0.166
Delta deep gray matter volume z-scores	0.08 ± 0.78	-0.01 ± 0.81	0.778
Delta white matter volume z-scores	0.05 ± 1.25	-0.43 ± 2.81	0.854

Abbreviations: EDSS = Expanded Disability Status Scale; F = female; IQR = interquartile range; M = male; MS = multiple sclerosis; PRL = paramagnetic rim lesion; SD = standard deviation; WM = white matter; NA = not available.

## Relationship Between PRLs and Brain Tissue Volume Changes Over Time

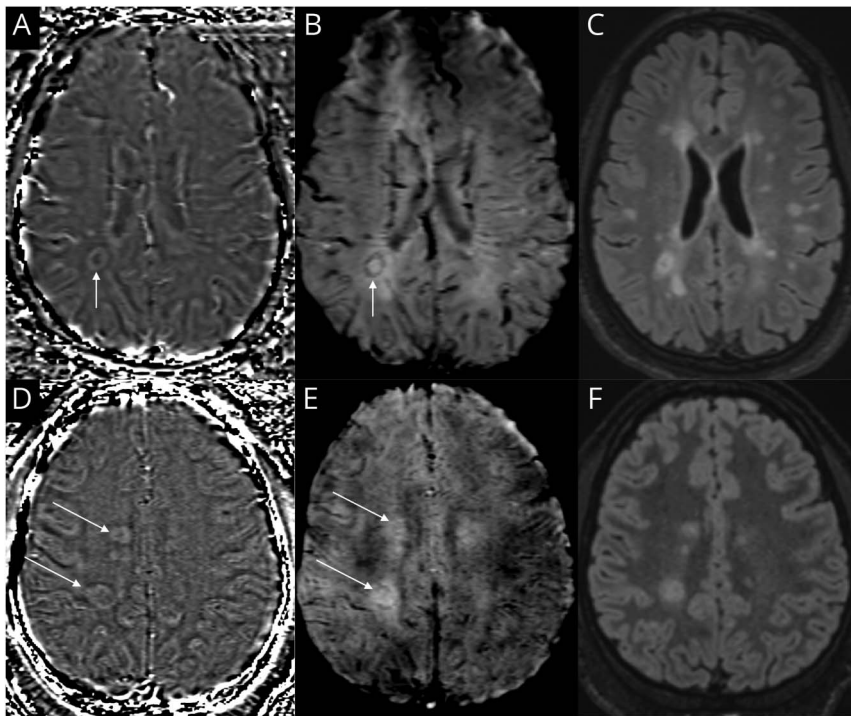
A time × PRL count interaction was observed for deep gray matter volume z-score ( $\beta = -0.021$ , 95% CI  $-0.035$  to  $-0.007$ ,  $p = 0.003$ ), indicating that higher PRL counts were associated with greater deep gray matter volume loss over time. No interactions were observed for clinical disability, cortical gray matter, white matter, or total brain volume (Table 3).

## Discussion

In this multicenter cross-sectional study of 54 patients with POMS, we observed a high prevalence of PRLs, with 74.1% of patients showing at least 1 PRL (median: 2 per patient). This is notably higher than reported in adult cohorts and consistent with prior pediatric studies showing a prevalence of 69%–92%.<sup>15–17</sup> PRLs were predominantly periventricular and

accounted for 25% of all WM lesions, twice the proportion seen in adult MS.<sup>12</sup> Clinical and radiologic disease activity and shorter disease duration were independent predictors of PRL count. Higher PRL count was associated with lower cortical and deep gray matter volume at baseline and with more severe deep gray matter volume loss over time.

The higher PRL prevalence in our study compared with adult cohorts, together with the finding that shorter disease duration independently predicted higher PRL count, suggests that PRL formation is an early event in the disease course. This is further supported by their association with more severe inflammatory activity, reinforcing the notion that PRLs may reflect heightened inflammation in the early stages of MS. While these findings contrast with those reported in adult MS, where PRLs have been more commonly associated with progressive disease,<sup>24,25</sup> they shed new light on the potential significance of these lesions, which may represent early-stage lesions characterized by



Panels A and D show SWI phase images (from a left-handed system) with white arrows indicating paramagnetic rim lesions (PRLs), characterized by hyperintense rims suggestive of iron-laden macrophage accumulation. Panels B and E display corresponding SWI images, also highlighting the peripheral hypointensity of PRLs with white arrows. Panels C and F present the fluid-attenuated inversion recovery (FLAIR) images, demonstrating hyperintense lesions at the same anatomical locations, consistent with chronic active demyelinating pathology. SWI = susceptibility-weighted imaging.

dynamic changes at their borders. Although we cannot determine whether these lesions represent more destructive, chronic inflammatory lesions linked to neurodegeneration,<sup>26</sup> the observed associations with gray matter atrophy suggest that PRLs may play a contributory role in longer term disability.

Of interest, we observed an inverse relationship between anti-CD20 therapy and PRL count. This finding supports the view that PRLs serve as markers of heightened inflammatory activity—given the well-known efficacy of anti-CD20 agents against acute inflammation<sup>27,28</sup>—and suggests that these treatments may also modulate the chronic evolution of inflammatory processes. However, the relatively limited number of patients receiving DMTs, and particularly anti-CD20 therapies, in this cohort precluded a more detailed investigation of their specific impact on the PRL-driven inflammation-neurodegeneration axis.

We found cross-sectional associations between PRL count and cortical gray matter volume, supporting the hypothesis of shared pathogenic mechanisms underlying these changes. While the available SWI sequences did not permit direct visualization of chronic inflammatory changes within cortical or deep gray matter, the observed volume loss may reflect such underlying pathology. The well-established relationship between lesion burden and thalamic atrophy in pediatric MS<sup>22,29</sup> suggests that PRLs, by virtue of their more destructive nature, could drive more severe antegrade and retrograde Wallerian degeneration, thereby contributing to greater gray matter

volume loss. Deep gray matter structures, particularly the thalamus, are highly interconnected and thus especially susceptible to secondary degeneration resulting from white matter injury. It is important to note that this association also persisted longitudinally, with higher PRL counts predicting more pronounced deep gray matter atrophy over time.

Despite the association between PRLs and more pronounced gray matter volume loss, we did not find any relationship between PRL count and EDSS scores. This aligns with prior pediatric MS studies reporting no association between high lesion load and early clinical disability,<sup>30</sup> potentially reflecting greater neuroplasticity or a delayed clinical manifestation of tissue damage in younger individuals.<sup>31,32</sup>

Nonetheless, PRLs may still carry prognostic value. In adult MS, their presence has been linked to future disability progression,<sup>24</sup> suggesting that the more severe gray matter atrophy observed in patients with higher PRL counts could ultimately contribute to earlier or more significant disability over time. However, PRLs likely represent only one aspect of a broader pathogenic process; although not sufficient on their own to account for disability, they may serve as valuable markers of compartmentalized tissue inflammation and ongoing neurodegeneration, also during the earliest stages of disease.

This study has several limitations. First, the limited follow-up duration and the minimal disability, which is frequently

**Table 2** Univariate Association With Paramagnetic Rim Lesion Count and Independent Associations Identified Through Stepwise Multivariable Poisson Regression Analysis

Univariate Poisson regression analysis			
	IRR	95% CIs	FDR-adjusted p values
Age	1.034	0.951–1.124	0.432
Sex	1.116	0.791–1.575	0.531
Disease duration	0.996	0.985–1.006	0.401
Number of relapses	1.007	0.865–1.173	0.924
T2-hyperintense lesion count	1.041	1.034–1.049	<0.001
T2-hyperintense lesion volume	1.029	1.018–1.040	<0.001
Brain volume z-score	0.909	0.850–0.973	0.006
Treatment with anti-CD20 vs no DMTs	0.640	0.447–0.917	0.015
<sup>a</sup> Other DMTs vs no DMTs	0.876	0.583–1.315	0.523
Multivariable stepwise Poisson regression analysis			
	IRR	95% CIs	p Value
Disease duration	0.987	0.975–0.999	0.035
T2-hyperintense lesion volume	1.018	1.004–1.032	0.012
T2-hyperintense lesion count	1.045	1.035–1.054	<0.001

Abbreviations: DMTs = disease-modifying treatments; EDSS = Expanded Disability Status Scale; FDR = false discovery rate; IRR = incidence rate ratio.  
<sup>a</sup>Other DMTs include any interferon-beta preparations and fingolimod.

observed in POMS, may have reduced our ability to detect significant changes in EDSS scores and brain tissue volumes. Second, the limited number of patients on DMTs constrained our capacity to investigate how these treatments influence PRL counts and their relationship with brain atrophy. Although the lack of postcontrast sequences could have led to an overestimation of PRLs, thereby biasing our prevalence and burden metrics, we restricted our analysis to scans acquired during clinical stability ( $\geq 4$  weeks after relapse), which should

largely attenuate this risk. Furthermore, owing to imaging artifacts, PRLs could not be reliably identified in infratentorial regions. Because the MRI scans were obtained during routine clinical care rather than through a controlled research protocol, there was no predefined interval from disease onset to the “baseline” scan. Instead, baseline was defined as the earliest scan that met our inclusion criteria, which could have introduced variability in the disease stage at the time of baseline assessment. The lack of an internal healthy control group limited our ability to account for scanner-related or protocol-related variability across sites. Moreover, although each patient underwent MRI on the same scanner throughout the follow-up period, multiple scanners were used within each center, resulting in only a limited number of patients per scanner. This limited the feasibility and statistical stability of including scanner as a random effect in our models. However, this is unlikely to have introduced systematic bias into our findings, particularly given the use of a validated segmentation technique designed to ensure reliable results across varying MRI contrasts and resolutions.<sup>2</sup>

Standard volumetric techniques were used to assess brain tissue integrity, but they may lack sensitivity to subtle or microstructural damage detectable with more advanced imaging modalities.<sup>33</sup> The absence of dedicated sequences, such as leptomeningeal contrast-enhanced FLAIR and multiecho SWI, also restricted our capacity to assess chronic inflammatory changes within the cortical gray matter, which may contribute to neurodegeneration in MS.<sup>34</sup>

In this multicenter study involving a relatively large cohort of patients with pediatric-onset MS, we confirmed that PRLs are more frequently observed in children and adolescents than in adults with MS, consistent with previous reports. Our findings also demonstrate that higher PRL counts correlate with greater inflammatory activity as proven by the association with T2-hyperintense lesion burden and more severe brain tissue loss, underlining their potential role as biomarkers of a more aggressive disease phenotype. By contrast, PRL count showed no association with current or short-term clinical disability, likely owing to

**Table 3** Brain Tissue Volume Changes Over the Follow-Up Period and Their Association With Paramagnetic Rim Lesion Count

	Time			Time*paramagnetic rim lesion count		
	$\beta$ coef	95% CIs	p Value	$\beta$ coef	95% CIs	p Value
EDSS scores	0.000	0.000–0.000	1.000	0.000	0.000–0.000	1.000
Brain volume z-scores	-0.342	-0.496 to -0.187	<0.001	-0.034	-0.070, 0.002	0.069
Deep gray matter volume z-scores	-0.127	-0.219 to -0.035	0.007	-0.021	-0.035, -0.007	0.003
Cortical gray matter volume z-scores	-0.266	-0.386 to -0.145	<0.001	-0.005	-0.033, 0.024	0.741
White matter volume z-scores	-0.156	-0.381 to 0.069	0.177	-0.029	-0.082, 0.024	0.284

Abbreviations: coef = coefficient; EDSS = Expanded Disability Status Scale.

preserved neuroplasticity and the early disease stage in this population. Taken together, these findings support the hypothesis that PRLs reflect sites of chronic neuroinflammation and may contribute to neurodegeneration over time. While clinical sequelae may not yet be apparent in pediatric patients, the strong relationship with tissue injury highlights the potential prognostic value of PRLs.

## Author Contributions

R. Nistri: major role in the acquisition of data; analysis or interpretation of data. E. De Meo: drafting/revision of the manuscript for content, including medical writing for content; analysis or interpretation of data. N.N. Kim: drafting/revision of the manuscript for content, including medical writing for content. V. Pozzilli: drafting/revision of the manuscript for content, including medical writing for content. P. Goebel: drafting/revision of the manuscript for content, including medical writing for content. M. Sa: drafting/revision of the manuscript for content, including medical writing for content. S. Ramdas: drafting/revision of the manuscript for content, including medical writing for content. A. Parida: drafting/revision of the manuscript for content, including medical writing for content. S. Wright: drafting/revision of the manuscript for content, including medical writing for content. E. Wassmer: drafting/revision of the manuscript for content, including medical writing for content. M. Eyre: drafting/revision of the manuscript for content, including medical writing for content. M. Lim: drafting/revision of the manuscript for content, including medical writing for content. T. Rossor: drafting/revision of the manuscript for content, including medical writing for content. C. Hemingway: drafting/revision of the manuscript for content, including medical writing for content. A. Biswas: drafting/revision of the manuscript for content, including medical writing for content. S. Sudhakar: drafting/revision of the manuscript for content, including medical writing for content. K. Mankad: drafting/revision of the manuscript for content, including medical writing for content. A. Eshaghi: drafting/revision of the manuscript for content, including medical writing for content. F. Barkhof: drafting/revision of the manuscript for content, including medical writing for content. O. Ciccarelli: drafting/revision of the manuscript for content, including medical writing for content. Y. Hachon: drafting/revision of the manuscript for content, including medical writing for content; study concept or design.

## Study Funding

The authors report no targeted funding.

## Disclosure

E. De Meo received speaker honoraria from Merck Serono and Novartis and served as advisor for BMS. K. Mankad has received personal fees from Cromwell Hospital, HCA United Kingdom, European Society of Paediatric Neuro-radiology, and United Kingdom Crown Court and acts as the Chair of the British Paediatric Neuroimaging Group outside the submitted work. F. Barkhof is part of the

steering committee or Data Safety Monitoring Board member for Biogen, Merck, ATRI/ACTC, and Prothena. He is a consultant for Roche, Celltrion, Rewind Therapeutics, Merck, IXICO, Jansen, and Combinostics. He has research agreements with Merck, Biogen, GE Healthcare, and Roche and is co-founder and shareholder of Queen Square Analytics Ltd; he reports consultancy fees from Roche, IXICO, and Combinostics; grants from Biogen (progressive multifocal leukoencephalopathy educational website); and personal fees from Merck (steering committee), Prothena (data and safety monitoring board membership), Biogen (steering committee), and Eisai (data and safety monitoring board membership) outside the submitted work. O. Ciccarelli is an NIH Research Professor (RP-2017-08-ST2-004); acts as a consultant for Biogen, Merck, Novartis, Roche, and Teva; and has received research grant support from the MS Society of Great Britain and Northern Ireland, the NIH UCLH Biomedical Research Centre, the Rosetree Trust, the National MS Society, and the NIH-HTA. All other authors report no relevant disclosures. Go to [Neurology.org/NN](http://Neurology.org/NN) for full disclosures.

## Publication History

Received by *Neurology*<sup>®</sup> *Neuroimmunology & Neuroinflammation* July 11, 2025. Accepted in final form September 17, 2025. Submitted and externally peer reviewed. The handling editor was Editor Scott S. Zamvil, MD, PhD, FAAN.

## References

1. Hachon Y, Banwell B, Ciccarelli O. What does first-line therapy mean for paediatric multiple sclerosis in the current era? *Mult Scler*. 2021;27(13):1970-1976. doi:10.1177/1352458520937644
2. Chitnis T, Aen G, Belman A, et al. Improved relapse recovery in paediatric compared to adult multiple sclerosis. *Brain*. 2020;143(9):2733-2741. doi:10.1093/brain/awaa199
3. Fadda G, Armangue T, Hachon Y, Chitnis T, Banwell B. Paediatric multiple sclerosis and antibody-associated demyelination: clinical, imaging, and biological considerations for diagnosis and care. *Lancet Neurol*. 2021;20(2):136-149. doi:10.1016/S1474-4422(20)30432-4
4. Aubert-Broche B, Fonov V, Narayanan S, et al. Onset of multiple sclerosis before adulthood leads to failure of age-expected brain growth. *Neurology*. 2014;83(23):2140-2146. doi:10.1212/WNL.0000000000001045
5. Yong HYF, Yong VW. Mechanism-based criteria to improve therapeutic outcomes in progressive multiple sclerosis. *Nat Rev Neurol*. 2022;18(1):40-55. doi:10.1038/s41582-021-00581-x
6. Klistorner S, Barnett MH, Yiannikas C, et al. Expansion of chronic lesions is linked to disease progression in relapsing-remitting multiple sclerosis patients. *Mult Scler*. 2021;27(10):1533-1542. doi:10.1177/1352458520974357
7. Calabrese M, Preziosa P, Scalfari A, et al. Determinants and biomarkers of progression independent of relapses in multiple sclerosis. *Ann Neurol*. 2024;96(1):1-20. doi:10.1002/ana.26913
8. Calvi A, Clarke MA, Prados F, et al. Relationship between paramagnetic rim lesions and slowly expanding lesions in multiple sclerosis. *Mult Scler*. 2023;29(3):352-362. doi:10.1177/13524585221141964
9. Calvi A, Carrasco FP, Tur C, et al. Association of slowly expanding lesions on MRI with disability in people with secondary progressive multiple sclerosis. *Neurology*. 2022;98(17):e1783-e1793. doi:10.1212/WNL.000000000000200144
10. Dal-Bianco A, Grabner G, Kronnerwetter C, et al. Slow expansion of multiple sclerosis iron rim lesions: pathology and 7 T magnetic resonance imaging. *Acta Neuropathol*. 2017;133(1):25-42. doi:10.1007/s00401-016-1636-z
11. Bagnato F, Hametner S, Yao B, et al. Tracking iron in multiple sclerosis: a combined imaging and histopathological study at 7 tesla. *Brain*. 2011;134(Pt 12):3602-3615. doi:10.1093/brain/awr278
12. Ng Kee Kwong KC, Mollison D, Meijboom R, et al. The prevalence of paramagnetic rim lesions in multiple sclerosis: a systematic review and meta-analysis. *PLoS One*. 2021;16(9):e0256845. doi:10.1371/journal.pone.0256845
13. Absinta M, Sati P, Masuzzo F, et al. Association of chronic active multiple sclerosis lesions with disability in vivo. *JAMA Neurol*. 2019;76(12):1474-1483. doi:10.1001/jamaneuro.2019.2399

14. Maggi P, Sati P, Nair G, et al. Paramagnetic rim lesions are specific to multiple sclerosis: an international multicenter 3T MRI study. *Ann Neurol.* 2020;88(5):1034-1042. doi:10.1002/ana.25877
15. Margoni M, Preziosa P, Storelli L, et al. Paramagnetic rim and core sign lesions in paediatric multiple sclerosis patients. *J Neurol Neurosurg Psychiatry.* 2023;94(10):873-876. doi:10.1136/jnnp-2022-331027
16. Sacco S, Virupakshaiah A, Papinutto N, et al. Susceptibility-based imaging aids accurate distinction of pediatric-onset MS from myelin oligodendrocyte glycoprotein antibody-associated disease. *Mult Scler.* 2023;29(14):1736-1747. doi:10.1177/13524585231204414
17. Micheletti L, Maldonado FR, Watal P, et al. Utility of paramagnetic rim lesions on 1.5-T susceptibility phase imaging for the diagnosis of pediatric multiple sclerosis. *Pediatr Radiol.* 2022;52(1):97-103. doi:10.1007/s00247-021-05188-4
18. Thompson AJ, Banwell BL, Barkhof F, et al. Diagnosis of multiple sclerosis: 2017 revisions of the McDonald criteria. *Lancet Neurol.* 2018;17(2):162-173. doi:10.1016/S1474-4422(17)30470-2
19. Bagnato F, Sati P, Hemond CC, et al. Imaging chronic active lesions in multiple sclerosis: a consensus statement. *Brain.* 2024;147(9):2913-2933. doi:10.1093/brain/awae013
20. Goebel P, Wingrove J, Abdelmannan O, et al. Enabling new insights from old scans by repurposing clinical MRI archives for multiple sclerosis research. *Nat Commun.* 2025;16(1):3149. doi:10.1038/s41467-025-58274-8
21. Evans AC; Brain Development Cooperative Group. The NIH MRI study of normal brain development. *Neuroimage.* 2006;30(1):184-202. doi:10.1016/j.neuroimage.2005.09.068
22. De Meo E, Meani A, Moiola L, et al. Dynamic gray matter volume changes in pediatric multiple sclerosis: a 3.5 year MRI study. *Neurology.* 2019;92(15):e1709-e1723. doi:10.1212/WNL.00000000000007267
23. Schabdach JM, Schmitt JE, Sotardi S, et al. Brain growth charts for quantitative analysis of pediatric clinical brain MRI scans with limited imaging pathology. *Radiology.* 2023;309(1):e230096. doi:10.1148/radiol.230096
24. Reeves JA, Mohebbi M, Wicks T, et al. Paramagnetic rim lesions predict greater long-term relapse rates and clinical progression over 10 years. *Mult Scler.* 2024;30(4-5):535-545. doi:10.1177/13524585241229956
25. Toru Asahina A, Lu J, Chugh P, et al. Prognostic significance of paramagnetic rim lesions in multiple sclerosis: a systematic review. *J Clin Neurosci.* 2024;129:110810. doi:10.1016/j.jocn.2024.110810
26. Krajnc N, Schmidbauer V, Leinkauf J, et al. Paramagnetic rim lesions lead to pronounced diffuse periplaque white matter damage in multiple sclerosis. *Mult Scler.* 2023;29(11-12):1406-1417. doi:10.1177/13524585231197954
27. Mar S, Valeriani M, Steinborn B, et al. Ocrelizumab dose selection for treatment of pediatric relapsing-remitting multiple sclerosis: results of the OPERETTA I study. *J Neurol.* 2025;272(2):137. doi:10.1007/s00415-024-12879-z
28. Hauser SL, Bar-Or A, Comi G, et al. Ocrelizumab versus interferon Beta-1a in relapsing multiple sclerosis. *N Engl J Med.* 2017;376(3):221-234. doi:10.1056/NEJMoa1601277
29. Mesaros S, Rocca MA, Absinta M, et al. Evidence of thalamic gray matter loss in pediatric multiple sclerosis. *Neurology.* 2008;70(13 Pt 2):1107-1112. doi:10.1212/01.wnl.0000291010.54692.85
30. Cera N, Pinto J, Faustino R. Functional and structural alterations in pediatric multiple sclerosis: a systematic review and a preliminary activation likelihood estimation functional magnetic resonance imaging meta-analysis. *Pediatr Rep.* 2025;17(3):57. doi:10.3390/pediatric17030057
31. Santoro JD, Waltz M, Aaen G, et al. Pediatric multiple sclerosis severity score in a large US cohort. *Neurology.* 2020;95(13):e1844-e1853. doi:10.1212/WNL.00000000000010414
32. Bartels F, Nobis K, Cooper G, et al. Childhood multiple sclerosis is associated with reduced brain volumes at first clinical presentation and brain growth failure. *Mult Scler.* 2019;25(7):927-936. doi:10.1177/1352458519829698
33. De Santis S, Granberg T, Ouellette R, et al. Evidence of early microstructural white matter abnormalities in multiple sclerosis from multi-shell diffusion MRI. *Neuroimage Clin.* 2019;22:101699. doi:10.1016/j.nicl.2019.101699
34. Makshakov G, Magonov E, Totolyan N, et al. Leptomeningeal contrast enhancement is associated with disability progression and grey matter atrophy in multiple sclerosis. *Neurol Res Int.* 2017;2017:8652463. doi:10.1155/2017/8652463